Energy-Efficient Video Transmission Over a Wireless Link

Ye Li, Martin Reisslein, *Senior Member, IEEE*, and Chaitali Chakrabarti, *Senior Member, IEEE*

Abstract—Energy minimization is an important design goal in wireless video transmission. We examine how the RF energy and the analog circuit energy, which account for a large part of the energy consumption for wireless video transmission, can be controlled with physical-layer parameters (e.g., modulation level, bit rate, bit error rate, and multiple access interference) and link-layer specifications (e.g., the buffer status, idle time, and active time). Building on these insights, we develop three energy-efficient video transmission schemes for the single-user system, i.e., frame-by-frame transmission, group of pictures (GOP)-by-GOP transmission, and client-buffer-related energy-efficient video transmission (CBEVT). Our simulations indicate that energy savings of up to 85% is achievable in the radio frequency (RF) front end using the CBEVT algorithm. We also present an energy-efficient optimal smoothing algorithm for reducing the RF front-end energy consumption and the peak data rate. For CDMA-based multiuser systems, we propose an RF front-end energy model that assumes perfect power control. We find the signal-to-interference-noise ratio (SINR) for the entire system that minimizes the total energy consumption. We propose the multiuser-based energy-efficient video transmission (MBEVT) algorithm, which can achieve energy savings of up to 38% for a six-user CDMA system with an independent 16-MB buffer for every uplink.

Index Terms—Energy efficiency, radio frequency (RF) front end, wireless video.

I. INTRODUCTION

WIRELESS multimedia services, which are growing in popularity, pose several challenges, including overcoming bandwidth variations and limited battery lifetime. Although the next-generation wireless technologies promise more reliable communication and higher bandwidth, the problem of high energy consumption during video transmission is largely unresolved. In this paper, we develop wireless video transmission schemes that ensure the timely delivery of the video frames while saving energy.

Y. Li was with the Department of Electrical Engineering, Arizona State University, Tempe, AZ 85287-5706 USA. He is now with the Institute of Biomedical and Health Engineering, Shenzhen Institutes of Advanced Technology, Chinese Academy of Sciences, Shenzhen 518067, China (e-mail: ye.li@sub.siat.ac.cn).

M. Reisslein and C. Chakrabarti are with the Department of Electrical Engineering, Arizona State University, Tempe, AZ 85287-5706 USA (e-mail: reisslein@asu.edu; chaitali@asu.edu).

Color versions of one or more of the figures in this paper are available online at http://ieeexplore.ieee.org.

Digital Object Identifier 10.1109/TVT.2008.927720

For the design of energy-efficient wireless video transmission schemes, the cause of the energy consumption needs to be better understood. For instance, the circuit energy in the radio frequency (RF) front end[1] can no longer be ignored. Consider the IEEE 802.11b wireless LAN card based on Intersil's PRISM II chipset that consumes about 110 mW for the medium access control (MAC) processor, 170 mW for the digital baseband electronics, 240 mW for the analog electronics, and 600 mW for the power amplifier (PA) [1]. Thus, about 75% of the total power is dissipated in the RF front-end circuit. To accurately evaluate the RF front-end energy consumption, we build on our RF front-end energy model work [2], [3] and tie the physical-layer (PHY) parameters [e.g., bit error rate (BER), modulation level, bandwidth, bit rate, and multiple access interference (MAI)] to the RF circuit energy consumption. Our video transmission schemes adjust these PHY parameters to minimize the RF energy consumption.

The low-power wireless video transmission schemes must also consider the video streaming quality-of-service (QoS) constraints. Our schemes explicitly consider video streaming parameters [e.g., the client/receiver buffer status, the permissible stream start-up delay, the varying video bit rates (encoded frame sizes), and the video frame playout deadlines] to ensure the timely delivery of the video frames.

There has not been much work on low-power video transmission. Kim and Kim [8] propose a power-distortion-optimized coding mode-selection scheme for variable-bit-rate (VBR) video over time-varying channels to minimize the transmit power subject to distortion constraints. The target BER of a video packet is variable and is determined by the importance of the packet. The authors also propose an optimum power management scheme over slowly varying Rayleigh fading channels [9].

Lu *et al.* [7] present a Reed–Solomon channel encoder power model, a block-based H.263 encoder power model, and a distortion model. They jointly optimize the transmission energy, the code rate of the channel encoder, and the source encoder for minimum power consumption in cellular networks. They further minimize the transmission power consumption over wireless local area networks by finding the optimal PHY and MAC parameters [10]. A two-step fast algorithm for reducing the computation burden in the base station for a multiuser environment has also been developed [11].

---

[1]We define the RF front-end as the building blocks after (and including) the digital-to-analog converter (DAC) in the transmitter and the blocks before (and including) the analog-to-digital converter (ADC) in the receiver.

Zhang *et al.* [12] propose a power-minimized bit-allocation scheme that jointly considers the processing power for source coding and channel coding, as well as the transmission power. The total bits are allocated between source and channel coders to minimize the total power consumption according to the wireless channel conditions and video quality requirement.

For high-quality video stream transmission, the peak data rate may exceed the nominal bandwidth over wireless links. In [13], Luna *et al.* propose a joint source coding and data rate adaptation method to minimize the transmission power under delay and quality constraints. Salehi *et al.* present an effective algorithm that achieves the largest possible reduction in the rate variability with a given buffer size [14]. However, their work ignores the energy consumption. In [15], Pollin *et al.* propose a cross-layer resource allocation method for multiuser scenario and evaluate the performance using MPEG-4 video traces. Yeh *et al.* [16] examine energy saving mechanisms (in particular, the impact of timer settings) in two major wireless standards.

One of the key limitations of existing works on low-power video delivery is that they focus on transmission energy but ignore or oversimplify the effect of the RF front-end circuit energy. The RF front end, however, consumes more dissipated energy than radiated energy because of the low efficiency of a class-A PA, particularly for communication over small or medium distances. In this paper, we develop new energy-efficient video transmission schemes that are based on an accurate system-level energy model for the RF front end [2], [3].

Our approach to designing energy-efficient video transmission schemes largely relies on adapting the modulation level while considering the related PHY parameters (e.g., bit rate, bandwidth, signal-to-noise ratio (SNR), and MAI) to reduce RF energy consumption. Related MAC layer parameters (e.g., the idle time and the active time of the transmitter) are also optimized for the lowest transceiver energy consumption. We schedule the data rate according to the buffer occupancy (i.e., the data-link layer) and the MPEG stream frame specifications (i.e., the application layer). Although source video coding also contributes to the energy consumption [7], we do not consider its effect in this paper. Our focus is on the energy-efficient transmission of preencoded video.

We develop several low-power video transmission schemes for a single-user wireless system. The frame-by-frame scheme and the group of pictures (GOP)-by-GOP scheme transmit at the optimal data rate for every frame or GOP and, thereby, save energy. The client-buffer-related energy-efficient video transmission (CBEVT) algorithm considers the effect of both the client buffer occupancy and the video delay constraint and is shown to have the highest RF energy savings. The modified optimal smoothing algorithm is an extension of the work in [14], which can reduce both the RF energy consumption and the peak data rate. We develop an RF front-end energy model for the code division multiple access (CDMA)-based multiuser system and propose a multiuser-based energy-efficient video transmission (MBEVT) algorithm. In this algorithm, the entire system energy consumption is minimized by considering the number of active users, client buffer sizes, and delays. The performance of these schemes is evaluated using 30-min MPEG-4 encodings with a range of bit rates.

The remainder of this paper is organized as follows. Section II describes the dominant power parameters for every RF component in the wireless transceiver and the operation modes for the RF transceiver. Section II also describes the notion of an optimal modulation level b and the parameters that affect it. The four low-power video transmission schemes for the single-user system are proposed in Section III, and their energy performance is evaluated. Section IV describes the improved RF front-end energy model for the multiuser environment, the MBEVT algorithm, and its energy performance. Section V summarizes this paper.

II. POWER MODEL AND OPERATION MODES FOR THE TRANSCEIVER

We consider a full-duplex transceiver for a CDMA-based wireless device in Wi-Fi networks. The receiver and the transmitter work independently. During communication, the transmitter delivers a video stream to the base station via the uplink, whereas the receiver gets the feedback and state information from the base station via the downlink. Uplink and downlink work at different data rates and at different modulation levels.

A. Transceiver Building Blocks

To minimize the total energy consumption for video transmission, it is essential to consider the energy consumption of the RF front end. We use the standard wireless transmitter and receiver model in [4], as described in Figs. 1 and 2, respectively. The main components of the analog signal chain of the transmitter are DAC, reconstruction filter, mixer, PA, and RF filter. Similarly, the main components of the receiver signal chain are the RF-band select filter, low-noise amplifier (LNA), downconversion mixers, baseband amplifier, baseband and antialiasing filter, ADC, and RF synthesizer.

B. Power Model of the RF Front End

We employ the power models in [2] and [3] for each of the components in the analog signal chain of a transmitter/receiver. These models have been derived by considering the dominant power parameters [e.g., the signal bandwidth, signal center frequency, signal peak-to-average ratio (PAR), modulation level, SNR, and gains].

Table I [2] summarizes the effects of the different parameters that contribute to the power consumption of the different RF front-end components. For instance, the power consumption of a class-A PA is a function of the PAR, distance d, number of bits per symbol b, and symbol error rate. Table I also lists the exemplary power consumption of the different RF components in the active mode.

C. Operation Modes of the RF Transceiver

In video transmission, the transceiver works in the following four modes:

1) *Transmit*. The transmitter is fully on. The transmitter modulates the data and sends it through the antenna.
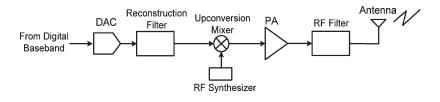
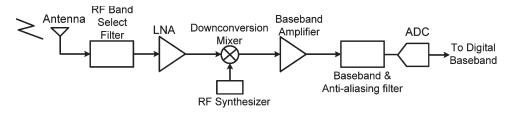Fig. 1. Block diagram of the transmitter analog signal chain.

Fig. 2. Block diagram of the receiver analog signal chain.

TABLE I
RF POWER CONSUMPTION FOR DIFFERENT BLOCKS IN
THE RF FRONT END OF A TRANSCEIVER IN [2]

Components	Power Model Parameters	Transmit Mode	Idle/Receive Mode
PA	*PAR, d, b, SER, R_s*	126.5 mW	0 mW
Mixer	*K,NF*	21 mW	21 mW
Freq. Syn.	*$\omega_c, F_{LO}, F_{ref}$*	67.5 mW	67.5 mW
LNA	*A, NF*	0 mW	20 mW
ADC	*PAR, SQNR, f*	0 mW	5.85 mW
DAC	*PAR, SQNR, OSR*	15.4 mW	0 mW
Filter	*f, SNR*	2.5 mW	2.5 mW
Baseband Amplifier	*B, α_{BA}*	0 mW	5 mW
Ref. System	*V_{dd}, I_{ref}*	0.5 mW	0.5 mW
Total	*N/A*	233.4 mW	122.35 mW

PAR is the peak-to-average ratio; *SNR* is the signal-to-noise ratio; *SER* is the symbol error rate; *d* is the transmission distance; *R_s* is the signal symbol rate; *b* is the modulation level (number of bits per symbol); *K* is the gain of the mixer; *NF* is the noise figure; *ω_c* is the center frequency of the VCO; *F_{LO}* is the frequency of the local oscillator; *F_{ref}* is the reference frequency; *A* is the gain of the LNA; *SQNR* is the signal-to-quantization noise ratio of the ADC and DAC; *f* is the signal frequency of the ADC; *OSR* is the over-sampling ratio of the DAC; *B* is the bandwidth of the baseband amplifier; *α_{BA}* is the gain of baseband amplifier; *V_{dd}* is the DC voltage; *I_{ref}* is the reference current. *P_{out_rms}*=13 dBm. We used *PAR*=5 dB, *d*=10 m, *b*=4 for calculating the exemplary PA transmit mode power in the table.

2) *Receive*. The receiver is fully on. The receiver detects, demodulates, and passes packets to the baseband processor.
3) *Idle*. Most blocks in the transmit signal chain are turned off, whereas the receiver is still on. The baseband processor is partially on.
4) *Transient mode*. The transmitter switches from the idle mode to the transmit mode, and *vice versa*.

We ignore the sleep mode, because the transceiver is hardly turned off during video transmission. The total energy con-

sumption in the RF front end is given by the sum of the energy consumption in the four modes, i.e.,

$$
E_{\text{total}} = P_{\text{transmit}} T_{\text{transmit}} + P_{\text{receive}} T_{\text{receive}}
$$
$$
+ P_{\text{idle}} T_{\text{idle}} + P_{\text{transient}} T_{\text{transient}}. \quad (1)
$$

In many state-of-the art analog and RF circuits, digital calibration and speed-up modes are used to quickly bring the front end to a fully operational mode, which makes the transient energy consumption $P_{\text{transient}} T_{\text{transient}}$ negligible. Furthermore, the idle power consumption in the RF front-end circuit is almost the same as that in the receive mode [2]; therefore, we approximate $P_{\text{idle}} \approx P_{\text{receive}}$. The entire RF circuit or parts of the RF circuit are turned on in the transmit, receive, and idle modes, so these three modes constitute the active mode, i.e., $T_{\text{active}} = T_{\text{transmit}} + T_{\text{receive}} + T_{\text{idle}}$. However, for a full-duplex system, the receive-mode time covers the transmit-mode time. Hence, $T_{\text{active}} = T_{\text{receive}} + T_{\text{idle}}$, and (1) can be simplified as

$$
E_{\text{total}} = E_{\text{transmit}} + E_{\text{receive}}
$$
$$
= P_{\text{transmit}} T_{\text{transmit}} + P_{\text{receive}} T_{\text{active}}. \quad (2)
$$

The transmit-mode energy consumption E_{transmit} can further be divided into 1) signal transmission energy (i.e., the radiated energy), which is delivered to the antenna, and 2) dissipated energy, which is the energy consumed by the electronic circuits. The transmission energy is delivered by the PA, so P_{PA} includes both radiated and dissipated energy [4], [5]. We have

$$
E_{\text{transmit}} = (P_{\text{PA}} + P_{\text{mix}} + P_{\text{FS}} + P_{\text{filter}} + P_{\text{DAC}}) T_{\text{transmit}}
$$

where P_{PA}, P_{mix}, P_{FS}, P_{filter}, and P_{DAC} are the power consumption of the PA, mixer, frequency synthesizer, analog filters, and DAC, respectively. In Section III, we discuss the transmit energy consumption in detail.

In the receive mode

$$
E_{\text{receive}} = (P_{\text{LNA}} + P_{\text{mix}} + P_{\text{FS}} + P_{\text{filter}} + P_{\text{BA}} + P_{\text{ADC}}) T_{\text{active}}
$$

where P_{LNA}, P_{BA}, and P_{ADC} are the power consumption of the LNA, baseband amplifier, and ADC, respectively. Based on Table I, most of the dominant power parameters in the receive signal chain (e.g., the operation frequency, the peak bandwidth, and the gain) cannot be adjusted during communication. Therefore, we consider the total power consumption in the receive mode as a constant, and the energy consumption is considered only as a function of the active time.

D. Energy Consumption in the Transmit Mode

As illustrated in Table I, the dominant power parameters for the mixer, frequency synthesizer, DAC, and analog filters are typically fixed. We consider a common scenario where the total power consumption of these blocks is fixed at 107 mW. Although the DAC is a PAR-related component, and, thus, the power consumption is related to the modulation level, the power variation in the DAC is comparatively small. Hence, we consider the DAC power consumption as a constant. However, the power consumption of the PA depends on adjustable parameters (e.g., d, PAR, R_s, and b), which allows us to select these parameters to minimize the transmission energy.

Consider M quadratic-amplitude modulation (M-QAM) and denote $T_{\text{bit}} = 1/(b \cdot R_s)$, where R_s is the symbol rate, in hertz. Then, the active energy consumption per bit for the RF front end for all modulation levels b is given by [2]

$$E_{\text{bit}} = \frac{107 \times 10^{-3}}{b \cdot R_s} + \frac{16\pi^2 d^2 L}{3 G_r G_t \lambda^2 K}(2^b - 1)N_0\frac{1}{b}$$

$$\cdot \left(Q^{-1}\left(\frac{1}{4}\left(1 - \frac{1}{2^{b/2}}\right)^{-1} b \cdot \text{BER} \right) \right)^2 \text{PAR}(b, \alpha) \quad (3)$$

where the first term $(107 \times 10^{-3})/(b \cdot R_s)$ is the energy of all components, except the PA, and the second term is the energy consumption of the PA. Q^{-1} is the inverse of the function $Q(x) = \int_x^\infty (1/\sqrt{2\pi})e^{-y^2/2}dy$. PAR is a function of the modulation level b and is also affected by the pulse-shaping roll-off factor α, which we fix to 0.25. Based on [2] and [3], we have

$$\text{PAR} = \sqrt{\frac{3 \cdot (2^{b/2} - 1)}{(2^{b/2} + 1)}} \cdot \text{PAR}_C \cdot \text{PAR}_{\text{roll-off}} \quad (4)$$

where PAR_c and $\text{PAR}_{\text{roll-off}}$ are the PAR of the carrier and the PAR that is related to the roll-off factor α, respectively. For a sine wave carrier, $\text{PAR}_c = 1.4$.

In the remaining parts of this section, we consider the system to have fixed bandwidth and a fixed symbol rate, which is very common in current wireless systems.

E. Optimal Modulation Level in a Fixed-Bandwidth System

In this section, we determine the *optimal* modulation level that minimizes the energy consumption per bit for fixed-bandwidth systems. To find the optimal modulation level b, we need to find the value of b for which $dE_{\text{bit}}/db = 0$. Finding the derivative of (3) is not straightforward; therefore, we make

TABLE II
SYSTEM PARAMETER VALUES FOR THE WI-FI APPLICATION FOR
DETERMINING THE OPTIMAL MODULATION LEVEL b

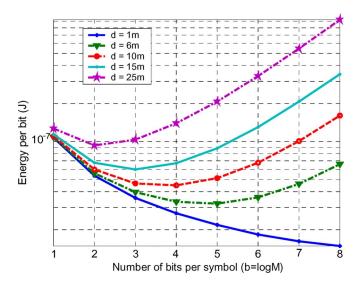|	
R_s=1MHz	G_r=1
G_t=1	L=0.8
f_c=2.5GHz	λ=0.12m
α=0.25	K=0.5
$N_0/2$=10^{-16}W/Hz	BER=10^{-3}
I_{0_DAC}=10 μA	$SQNR_{ADC}$=50dB
$SQNR_{DAC}$=60dB	OSR_{DAC}=4

Fig. 3. RF front-end active energy per bit versus modulation level b with different distance d (PAR = 5 dB, and BER = 10^{-3}).

use of fourth-order regression to approximate the second term in (3). Furthermore, we set the BER and other system parameters, as listed in Table II, and establish a relationship between b, R_s, and d, i.e.,

$$E_{\text{bit}} = \frac{107 \times 10^{-3}}{b \cdot R_s} + \frac{16\pi^2 d^2 L}{3 G_r G_t \lambda^2 K} N_0 \cdot \text{PAR}_{\text{roll-off}} \cdot \text{PAR}_C$$

$$\times (0.4008b^4 - 5.1513b^3 + 29.3804b^2 - 63.1092b + 68.2878). \quad (5)$$

Let $C_1 = 107 \times 10^{-3}$ and $C_2 = (16 \cdot \pi^2 \cdot L \cdot N_0 \cdot \text{PAR}_{\text{roll-off}} \cdot \text{PAR}_c)/(3 G_r G_t \lambda^2 K) = 3.269 \times 10^{-12}$. Then, $dE_{\text{bit}}/db = 0$ implies

$$1.6032b^5 - 15.4539b^4 + 58.7608b^3 - 63.1092b^2 - \frac{C_1}{R_s \cdot C_2 d^2} = 0. \quad (6)$$

Solving (6) for b gives the optimal b, which is a function of d. Although the optimal b is also affected by the parameters R_s, N_0, λ, α, G_r, and G_t, these are typically fixed or have negligible effects on b and are considered constant in this analysis.

Fig. 3 describes the effect of the modulation level b on E_{bit} for different values of the distance d. We observe that, for every d, there is a modulation level b for which E_{bit} is minimal, i.e., b_{opt}. For instance, for $d = 1$ m, $b_{\text{opt}} = 8$, and for $d = 6$ m, $b_{\text{opt}} = 5$. When b is less than b_{opt}, the RF front-end energy consumption reduces with the increase in b, because, for small b, the energy consumption of other RF front-end components,

except for the PA [i.e., the first item in (5)], are dominant. For b larger than b_{opt}, the energy that is consumed in the PA [i.e., the second item in (5)] is dominant, and the RF front-end energy increases with b. (If we plotted the modulation level for values that are higher than 8, the curve for $d = 1$ m would show the same tendency as other curves.) For larger b, the signal is more susceptible to interference, and higher PA radiated power is necessary to maintain the BER. A similar trend can also be seen in [2]. In typical wireless environments, modulation levels b of 8 or higher are impractical; therefore, we focus on the energy performance in the range 1–8. For a fixed d, the observed E_{bit} trends are similar to those in [5] and [18]. When the transmission distance is low, [5] and [18] show that E_{bit} decreases as b increases for a small b and, then, increases for a larger b.

Fig. 3 also shows that the value of b_{opt} decreases as d increases. The energy consumption of the PA is d sensitive, so a larger d means higher energy consumption of the PA, which compensates for the path loss of the signal and maintains the BER, thus resulting in a smaller b_{opt}.

III. ENERGY-EFFICIENT VIDEO TRANSMISSION FOR A SINGLE-USER COMMUNICATION SYSTEM

We consider VBR-encoded video streams, where the frame size (in bits) is variable, and the frame period is typically fixed. In this paper, we use a typical frame period of 33 ms. We propose four adaptive video transmission schemes: 1) frame-by-frame transmission; 2) GOP-by-GOP transmission; 3) CBEVT; and 4) an energy-efficient optimal smoothing scheme. Consistent with typically rare mobility when watching videos in Wi-Fi networks, we consider a slow-fading channel in which the attenuation factor is constant over the duration of a frame or GOP. Although the optimal modulation level b_{opt} infrequently changes for the considered largely stationary Wi-Fi video scenario, our algorithms, in principle, require that the parameters that affect the optimal modulation level, including the distance and channel conditions, are frequently updated such that the currently valid optimal modulation level is available when our transmission schemes make decisions on the modulation level that is used for the transmission of a video frame (or GOP), i.e., every video frame period (or GOP). The basic idea of our adaptive transmission schemes is to adjust the modulation level b (and, correspondingly, the data transmission rate) for every video frame (or GOP) to save energy. Thus, our transmission schemes require that the wireless system can change the modulation level every video frame period (or GOP). Most current wireless systems (e.g., wideband CDMA and 802.11) can easily meet these update frequency requirements. We also require that the underlying optimal modulation level rarely changes while the transmission of a given video frame (or GOP) is ongoing, which is reasonable for video reception in Wi-Fi networks with rare mobility. (Slight channel variations during an ongoing frame transmission could be compensated by automatic gain control.)

We compare the performance of our adaptive transmission schemes with respect to a baseline transmission scheme, which transmits the video frames without any adjustment. Baseline transmission uses 16-QAM and transmits each frame with the fixed modulation level $b = 4$, which is large enough to transmit the largest video frame within one video frame period of 33 ms (for smaller frames, the transmitter finishes the transmission before the end of the video frame period and, then, becomes idle until the end of the video frame period). We evaluate the performance of our schemes for different data rates, client (receiver) buffer sizes, and start-up delays.

We set the BER to 10^{-3} and suppose that nonadaptive forward error control (FEC) can correct this level of bit error such that there is no frame loss. (Note that the FEC is only one of the many functions that are carried out in the digital baseband processor, which consumes significantly less power than the RF front end [1]. Hence, the power consumption for the FEC can be considered a small constant and is ignored in this work.)

In this section, we consider a single ongoing video stream transmission. Multiple simultaneously ongoing video stream transmissions in a wireless CDMA system are considered in Section IV. For wireless TDMA systems that need to support multiple stream transmissions in a given frequency band, the transmissions for the different ongoing video streams need to be separated in time. Real-time transmissions schemes, e.g., [19]–[22], can achieve this transmission time separation and ensure that the video packets are delivered with minimal delay. Such real-time schemes can be combined with the single-stream energy-saving transmission schemes that were developed in this section: evaluating the combinations of the energy-saving transmission schemes with real-time transmission schemes are beyond the scope of this paper and are an interesting direction for future work.

Knowing the client buffer capacity, the transmitter keeps track of the client buffer occupancy by tracking its transmissions and the size of the video frames that were retrieved from the buffer for playout according to the fixed known playout schedule of the preencoded video. In a system with frame loss on the wireless link, an acknowledgment/negative acknowledgment mechanism would be necessary so that the transmitter can track the successfully received video frames. In addition, note that, in a system with frame loss, for a fixed BER, which we achieve by adjusting the modulation level and the transmission power, the frame loss and retransmission rates are constant for different modulation levels, which allows us to ignore the retransmission energy consumption.

A. Frame-by-Frame Transmission

A given frame is transmitted within one frame period. Let b_{req} be the required modulation level to transmit the frame in one frame period. If b_{req} is smaller than b_{opt}, we choose b_{opt} as the modulation level; if b_{req} is larger than b_{opt}, we use b_{req}. When b_{opt} is chosen for low-power transmission, the data rate increases, and the frame is transmitted in a shorter time, i.e., within less than the 33-ms frame period. After the transmission, the transmitter goes to the idle mode for the remainder of the frame period, and only the receiver is in operation.

B. GOP-by-GOP Transmission

In an MPEG video stream, several frames make up one GOP. In this work, we assume that 12 frames make up one

GOP. We can treat one GOP as a large frame and transmit it with a lower energy. Suppose that for frame n, T_n, l_n, and b_n are the time duration, frame size (in bits), and modulation level, respectively. In addition, let $e(T_n)$ denote the energy consumption for frame n; $E(b_n)$ is the energy consumption for frame n with modulation level b_n. Let R_b and R_s denote the bit rate and the symbol rate, respectively. The optimization constraints and the objective function can be stated as follows:

Constraints

1) $T_1 + T_2 + T_3 + \cdots + T_{12} <= T$ (preset deadline $=$ 396 ms).
2) $T_n = T_{\mathrm{bit}} \times l_n = l_n/R_b = l_n/b_n \cdot R_s$.

Objective function: $\min_{\{T_i\}}(\sum_{i=1}^{12} e(T_i))$.

Based on the first two constraints, we have

$$\sum_{n=1}^{12} \frac{l_n}{b_n} \leq T \cdot R_s.$$

The objective function can be restated as

$$\min_{\{T_i\}} \left(\sum_{i=1}^{12} e(T_i) \right) = \min_{\{b_n\}} \left(\sum_{n=1}^{12} E(b_n) \right).$$

Using the RF energy model in (5), we define $P = C_1/R_s$, $M = C_2 \cdot d^2$, and $f(b) = 0.4b^4 - 5.15b^3 + 29.38b^2 - 63.11b + 68.29$. Then, (5) can be expressed as

$$E_{\mathrm{bit}} = \frac{P}{b} + M \times f(b).$$

Hence, the objective function is

$$\min_{\{b_n\}} \sum_{n=1}^{12} \left(P \times \frac{l_n}{b_n} + M \times f(b_n) \times l_n \right)$$

$$\text{such that} \qquad \sum_{n=1}^{12} \frac{l_n}{b_n} \leq T \cdot R_s. \qquad (7)$$

The corresponding Lagrangian is

$$y = \sum_{n=1}^{12} \left(P \times \frac{l_n}{b_n} + M \times f(b_n) \times l_n \right) + \mu \cdot \left(\sum_{n=1}^{12} \frac{l_n}{b_n} - T \cdot R_s \right)$$

where $\mu \geq 0$ is the Lagrange multiplier.

For a local minimum, the first-order necessary condition is

$$\frac{\partial y}{\partial b_n} = -\frac{P}{b_n^2} + M \times f'(b_n) - \frac{\mu}{b_n^2} = 0. \qquad (8)$$

We have the following two possibilities:

1) The constraint is inactive, i.e., $\sum_{n=1}^{12} (l_n/b_n) < T \cdot R_s$ and $\mu = 0$. This constraint maps to solving a problem without constraints. Equation (8) reduces to $-(P/b_n^2) + M \times f'(b_n) = 0$, which can be expressed as

$$1.6b_n^5 - 15.45b_n^4 + 58.76b_n^3 - 63.11b_n^2 - \frac{P}{M} = 0. \qquad (9)$$

TABLE III
OOPTIMAL MODULATION LEVELS b_{opt} FOR DIFFERENT TRANSMISSION DISTANCES d

d (m)	b_{opt}
3	6
10	4
15	3
25	2

Although the fifth-order equation has five roots, there is only one real root that is the optimal modulation level b_{opt}. Note that b_{opt} is a function of d, because P/M is a function of d. We list some typical d values and the corresponding real roots in Table III.

2) The constraint is active, i.e., $\sum_{n=1}^{12} (l_n/b_n) = T \cdot R_s$. The objective function (7) becomes

$$\min_{\{b_n\}} \left(P \cdot T \cdot R_s + \sum_{n=1}^{12} M \cdot f(b_n) \cdot l_n \right).$$

The first-order necessary condition is

$$M \times f'(b_n) - \frac{\mu}{b_n^2} = 0, \qquad n = 1, 2, \dots, 12$$

$$1.6b_n^5 - 15.45b_n^4 + 58.76b_n^3 - 63.11b_n^2 - \frac{\mu}{M} = 0. \qquad (10)$$

In (10), $b_n^2 \times f'(b_n)$ is positive and monotonically increases with integer b for any $b > 1$. μ and M are positive, so (10) has only one real root. The optimal modulation levels are, thus, the same for all n, and $b_n^* = \sum_{n=1}^{12} l_n/(T \cdot R_s)$.

The final modulation level b_n^* can be calculated as follows. We first check whether $\sum_{n=1}^{12} (l_n/b_{\mathrm{opt}}) < T \cdot R_s$. If it is true, $b_n^* = b_{\mathrm{opt}}$; otherwise, $b_n^* = \sum_{n=1}^{12} l_n/(T \cdot R_s)$. ∎

Based on this analysis, we find that transmitting all the frames in one GOP with the same modulation level b is the most energy-efficient scheme. The GOP-by-GOP scheme is summarized as follows:

GOP-by-GOP Transmission
1. Choose b_{opt} for distance d according to (9);
2. Check whether $\sum_{n=1}^{12} (l_n/b_{\mathrm{opt}}) < T \cdot R_s$.
   If it is true, $b_n^* = b_{\mathrm{opt}}$ until 12 frames of GOP are transmitted. Then, idle the transmitter for the remainder of the GOP period.
   Else, $b_n^* = \sum_{n=1}^{12} l_n/(T \cdot R_s)$ for all n.
3. End.

C. CBEVT Algorithm

Frame-by-frame and GOP-by-GOP transmission do not consider the effect of the client (receiver) buffer size and client buffer occupancy. However, in practical systems, the client buffer occupancy is one of the most important factors to help ensure good communication quality. For example, if the client buffer overflows, the lost frames have to be unnecessarily
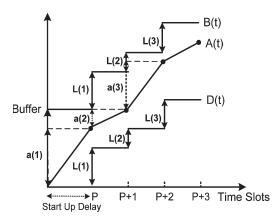
Fig. 4. Video data that the client received and consumed.

retransmitted, thus increasing the network load. On the other hand, in case of buffer starvation, frames are lost for uninterrupted playback, and the video must be suspended. In this section, we present the CBEVT scheme to avoid the client buffer from overflowing or starving while saving energy.

Algorithm Parameter Definition

N Number of frames in the video.

P Start-up delay in frame periods (time slots).

$Buffer$ Client buffer capacity for storing unplayed video frames.

$L(t)$ Size of frame in time slot t in bits ($t = 1, 2, \ldots N$).

$D(t)$ Cumulative amount of data (in bits) that the client consumed over $[1, t] : \sum_{i=l}^{t} L(i)$.

$a(t)$ Amount of data (in bits) that the transmitter transmitted during time slot t.

$A(t)$ Cumulative amount of data that was transmitted over $[1, t] : \sum_{i=l}^{t} a(i)$.

$B(t)$ Maximum cumulative data that can be received over $[1, t]$ without any buffer overflow.

C_{opt} Transmission rate that minimizes the RF energy per bit, $= b_{\text{opt}} \times R_s$, where R_s is the symbol rate.

Fig. 4 illustrates the variation in the amount of data in the client buffer over multiple time slots. The difference between $B(t)$ and $D(t)$ is the client buffer size. The cumulative data that was transmitted $A(t)$ must be more than $D(t)$ but less than $B(t)$ to ensure that the client buffer neither overflows nor starves. In every time slot, we can adjust $a(t)$ for energy minimization. Since $a(t) = b \times R_s \times T_{\text{frame}}$, there is a range of allowable modulation levels b. Using Fig. 3, we can select the value of b in this allowable range, which corresponds to the minimum E_{bit}. For example, if the start-up delay is $P(P \geq 1)$ time slots, the cumulative data that was transmitted by the end of the Pth time slot $A(P)$ should be larger than the size of the first frame $L(1)$ but smaller than the client buffer size, i.e., $L(1) \leq A(P) \leq Buffer$. In this range, we can choose the optimal $A(P)$ to minimize the energy consumption.

By the end of the $(P + 1)$th time slot, the transmitted data $A(P) + a(P + 1)$ should be more than the sum of the first two frames but smaller than the sum of the buffer size and the first frame, i.e., $L(1) + L(2) \leq A(P) + a(P + 1) \leq Buffer + L(1)$. When solving this inequality, $A(P)$ can be viewed as a constant, because it has already been determined

by the energy minimization for the previous P time slots, and we can adjust $a(P + 1)$ for the lowest energy consumption.

More generally, at the end of the $(P + k)$th time slot, $A(P), a(P + 1), a(P + 2), \ldots, a(P + k - 1)$ are treated as constants, and $a(P + k)$ is adjusted to minimize the energy consumption, i.e.,

$$\sum_{i=1}^{k+1} L(i) \leq A(P + k - 1) + a(P + k) \leq Buffer + \sum_{i=1}^{k} L(i) \quad (11)$$

from which we find that $a(P + k) = 0$ can satisfy the inequality if $A(P + k - 1) - \sum_{i=1}^{k+1} L(i) \geq temp$, where temp is a constant. Although temp $= 0$ satisfies the inequality, to avoid unexpected frame loss, we can set temp to be equal to the sum of several frame sizes to have a safety buffer of prefetched frames that allows continuous playback during wireless outages.

On the other hand, if $Buffer + \sum_{i=1}^{k} L(i) \leq A(P + k - 1) + C_{\text{opt}} \times T_{\text{frame}}$, then $a(P + k) \leq C_{\text{opt}} \times T_{\text{frame}}$, and the corresponding modulation level is smaller than the optimal b_{opt}, which is not energy efficient. Thus, if the transmitter is idle in this time slot but transmits a video with b_{opt} in the next time slot, the energy consumption can be reduced. Based on this insight, we propose the CBEVT algorithm as we have previously specified. CBEVT has superior performance compared to the frame-by-frame and GOP-by-GOP transmission. It not only has lower energy consumption but also reduces the peak data rate.

CBEVT function: find optimal schedule $(a(t), Buffer, P)$.

1. $T_{frame} = 33 \times 10^{-3}$ sec; $C_{opt} = b_{opt} \times R_s$; $temp = constant$; /* $temp \geq 0$

2. $a(1 : P) = C_{opt} \times T_{\text{frame}}$ /* P is the start-up delay

3.   IF $\sum_{i=1}^{P} a(i) \leq L(1)$/* video transmission during start-up delay

4. $a(1 : P) = L(1)/P$

5.   END IF

6.   IF $\sum_{i=1}^{P} a(i) \geq Buffer$

7. $Num = floor\lfloor Buffer/C_{opt} \times T_{frame} \rfloor$

8. $a(Num + 1) = Buffer - Num \times C_{opt} \times T_{frame}; a(Num + 2 : P) = 0;$

9.   END IF

10. $k = 0$

11.   Repeat /* video transmission begin at $(P + k)$th time slot

12. $k = k + 1$

13.   IF $\sum_{i=1}^{k+1} L(i) \leq \sum_{i=1}^{P+k-1} a(i) + C_{opt} \times T_{frame} \leq Buffer + \sum_{i=1}^{k} L(i)$

14.   OUTPUT frame $\langle a(k), C_{opt} \rangle$

15.   ELSE IF $\sum_{i=1}^{P+k-1} a(i) + C_{opt} \times T_{frame} < \sum_{i=1}^{k+1} L(i)$

16.   OUTPUT frame $\left\langle a(k), \dfrac{(\sum_{i=1}^{k+1} L(i) - \sum_{i=1}^{P+k-1} a(i))}{T_{frame}} \right\rangle$

17.   ELSE $(\sum_{i=1}^{k+1} L(i) \leq Buffer + \sum_{i=1}^{k} L(i) <$

         $\sum_{i=1}^{P+k-1} a(i) + C_{opt} \times T_{frame})$

18.   IF $\sum_{i=1}^{P+k-1} a(i) - \sum_{i=1}^{k+1} L(i) \geq temp$

19.   OUTPUT frame $\langle a(k), 0 \rangle$

20.   ELSE   OUTPUT   frame

         $\left\langle a(k), \dfrac{Buffer + (\sum_{i=1}^{k} L(i) - \sum_{i=1}^{P+k-1} a(i))}{T_{frame}} \right\rangle$

21.   END IF

22.   END IF

23.   UNTIL $k = N$

24.   END Function

Given the client buffer size, bit rate, and video delay constraint, we next show that the CBEVT algorithm is the most energy-efficient scheme. In the CBEVT algorithm, if $a(P + k)$ is smaller than the optimal data rate $C_{opt} = b_{opt} \times R_s$, and there is a sufficient number of video frames in the client buffer to continue video playback for $(temp + 1)$ time slots, we set $a(P + k) = 0$ and idle the transmitter for one or more time slots until the following video frames can be delivered at the optimal data rate. The question follows: Can we guarantee that the frames will be delivered at the optimal data rate, even after idling?

Inequality (11) shows that the optimal data rate is related to the client buffer size. We proceed to finding the necessary client buffer size, which guarantees that the transmitter can work at the optimal data rate after idling. Suppose that, at the $(P + k)$th time slot, both the constraints $A(P + k - 1) - \sum_{i=1}^{k+1} L(i) \geq temp$ and $Buffer + \sum_{i=1}^{k} L(i) \leq A(P + k - 1) + C_{opt} \times T_{frame}$ are satisfied. Then, we can set $a(P + k) = 0$. Thus

$$\sum_{i=1}^{k+1} L(i) \leq A(P + k - 1) + 0 \leq Buffer + \sum_{i=1}^{k} L(i)$$

$$\leq A(P + k - 1) + C_{opt} \times T_{frame}. \tag{12}$$

At the next time slot $(P + k + 1)$, if the constraints $A(P + k) - \sum_{i=1}^{k+2} L(i) \geq temp$ and $Buffer + \sum_{i=1}^{k+1} L(i) \leq A(P + k) + C_{opt} \times T_{frame}$ (where $A(P + k) = A(P + k - 1)$, because $a(P + k) = 0$) are still true, we can set $a(P + k + 1) = 0$. This step can be repeated until the constraints are violated. Let us assume that the two constraints are violated at the $(P + k + n)$th $(n \geq 1)$ time slot. If the transmission data rate at the $(P + k + n)$th time slot is not the optimal rate C_{opt}, we have one of the following two cases.

Case 1)   The amount of consumed data $\sum_{i=1}^{k+n+1} L(i)$ is larger than the amount of data that was transmitted with the optimal rate C_{opt}, i.e.,

$$A(P + k + n - 1) + C_{opt} \times T_{frame} \leq \sum_{i=1}^{k+n+1} L(i). \tag{13}$$

Since $a(P + k) = a(P + k + 1) = \cdots = a(P + k + n - 1) = 0$, we have

$$A(P + k + n - 1) + C_{opt} \times T_{frame}$$
$$= A(P + k + n - 2) + C_{opt} \times T_{frame} = \cdots$$
$$= A(P + k) + C_{opt} \times T_{frame}$$
$$= A(P + k - 1) + C_{opt} \times T_{frame}$$
$$\geq Buffer + \sum_{i=1}^{k+n} L(i) \geq \cdots \geq Buffer + \sum_{i=1}^{k} L(i).$$

Combined with (13), we have $Buffer + \sum_{i=1}^{k+n} L(i) \leq \sum_{i=1}^{k+n+1} L(i)$. Thus

$$Buffer \leq L(k + n + 1). \tag{14}$$

We, thus, conclude that if (13) holds, (14) holds. Thus, if we set the client buffer size to be larger than the maximum frame size, this case can be avoided.

Case 2)   The client buffer is overflowing if the transmission data rate is the optimal rate, i.e.,

$$A(P + k + n - 1) + C_{opt} \times T_{frame} \geq Buffer + \sum_{i=1}^{k+n} L(i). \tag{15}$$

Here, the constraint $A(P + k + n - 1) - \sum_{i=1}^{k+n+1} L(i) \geq temp$ must be false; otherwise, $a(P + k + n) = 0$. Therefore, $A(P + k + n - 1) < \sum_{i=1}^{k+n+1} L(i) + temp$, which implies

$$Buffer \leq A(P + k + n - 1) + C_{opt} \times T_{frame} - \sum_{i=1}^{k+n} L(i)$$

$$< \sum_{i=1}^{k+n+1} L(i) + temp + C_{opt} \times T_{frame} - \sum_{i=1}^{k+n} L(i).$$

Thus

$$Buffer < temp + C_{opt} \times T_{frame} + L(k + n + 1). \tag{16}$$

We, thus, conclude that if (15) holds, then (16) also holds. Thus, if the client buffer size is larger than two times, with temp $= 0$, the maximum frame size, this case can be avoided.

Based on the analysis of the two cases, we see that, if the client buffer size is larger than twice the maximum frame size, the data can be transmitted with the optimal modulation level b_{opt} while avoiding starvation and buffer overflow. Transmission at the optimal modulation level corresponds to the minimal energy consumption; therefore, we conclude that our CBEVT algorithm minimizes energy consumption.

D. Energy-Efficient Optimal Smoothing Algorithm

Although the CBEVT algorithm is guaranteed to be energy efficient, it has a relatively high peak data rate and requires a

large buffer. This may be unsuitable in narrowband communication systems with small client buffers. To reduce the peak bandwidth, the optimal smoothing algorithm has been proposed in [14]. The optimal smoothing algorithm reduces the peak data rate in video transmission and avoids the overflow and starvation in the client buffer. In this section, we propose an energy-efficient optimal smoothing algorithm that improves the energy performance of the optimal smoothing algorithm.

Algorithm Parameter Definition

$B(t)$ $= \min\{D(t-1)+Buffer, D(N)\}$ for $t = 2, \ldots, N$, $B(1) = Buffer$.

$C_{\max}$ Maximum transmission rate over a given interval $[t_1, t_2]$ without overflowing the client buffer.

$C_{\min}$ Minimum transmission rate over a given interval $[t_1, t_2]$ without starving the client buffer.

t_B Is the latest time that the client buffer becomes full for initial buffer occupancy q when the transmitter sends at rate $C_{\max}$ over time interval $[t_1, t_2]$.

t_D Is the latest time that the client buffer becomes empty for initial buffer occupancy q when the transmitter sends at rate $C_{\min}$ over time interval $[t_1, t_2]$.

The other parameters, i.e., N, $Buffer$, $L(t)$, $D(t)$, $a(t)$, $A(t)$, and C_{opt}, are the same as in Section III-C.

The optimal smoothing algorithm in [14] relies on two insights: 1) the constant bit rate (CBR) transmission is as smooth as possible, so the smoothing algorithm must make the CBR transmission segments as long as possible and 2) if the client buffer is close to overflowing or starvation, the transmission rate ($C_{\max}$ and $C_{\min}$) must be changed as early as possible, which ensures that the rate change is as small as possible.

Now, if the energy consumption is also considered in the optimal smoothing algorithm, then we select the data rate in the range of $[C_{\min}, C_{\max}]$, which minimizes the energy consumption. In Fig. 3, we find that, if C_{opt} is between $C_{\max}$ and $C_{\min}$, the video segment can be transmitted at C_{opt}, which results in the minimum RF energy. If C_{opt} is larger than $C_{\max}$, the video segment has to be transmitted at $C_{\max}$ to avoid client buffer overflow. If C_{opt} is smaller than $C_{\min}$, the video segment transmission rate is $C_{\min}$ to avoid client buffer starvation. This step ensures that the total energy consumption is minimized, whereas the buffer neither overflows nor starves.

Energy-efficient optimal smoothing algorithm: Function: find the optimal schedule $(a(t), Buffer)$

1. $t_s = 0$, $t_e = 1$, $q = 0$; $C_{\max} = Buffer$, $t_B = 1$, $C_{\min} = L(1)$, $t_D = 1$
2.   Repeat
3.   Set $t_e^* = t_e + 1$
4.   IF $C_{\max} < \frac{D(t_e^*) - (D(t_s) + q)}{t_e^* - t_s}$, end segment at t_B:
5.   IF $C_{\max} \geq C_{\mathrm{opt}} \geq C_{\min}$
6.   OUTPUT segment $\langle t_B - t_s, C_{\mathrm{opt}} \rangle$
7.   ELSE IF $C_{\max} \geq C_{\min} \geq C_{optimal}$
8.   OUTPUT segment $\langle t_B - t_s, C_{\min} \rangle$
9.   ELSE ($C_{\mathrm{opt}} \geq C_{\max} \geq C_{\min}$)
10.   OUTPUT segment $\langle t_B - t_s, C_{\max} \rangle$
11.   END IF
12.   Start a new segment at t_B: $t_S = t_B$, $t_e = t_B + 1$, $q = B(t_B) - D(t_B)$

TABLE IV
CHARACTERISTICS OF THE VIDEO THAT WAS USED IN THE SIMULATION

	Stream 1	Stream 2	Stream 3	Stream 4
I-P-B Quant. Scale	30-30-30	06-08-10	04-04-04	04-04-04
Peak-to-Mean Ratio	8.42	14.22	11.7	4.78
Mean Bit Rate (Mbps)	0.0588	0.1231	0.2696	1.674
Peak Bit Rate (Mbps)	0.4951	1.7498	3.156	8.0

13.   ELSE IF $C_{\min} > \frac{B(t_e^*) - (D(t_s) + q)}{t_e^* - t_s}$, OR, $t_e^* = N$ end the segment at t_D:
14.   IF $C_{\max} \geq C_{\mathrm{opt}} \geq C_{\min}$
15.   OUTPUT segment $\langle t_D - t_s, C_{\mathrm{opt}} \rangle$
16.   ELSE IF $C_{\max} \geq C_{\min} \geq C_{\mathrm{opt}}$
17.   OUTPUT segment $\langle t_D - t_s, C_{\min} \rangle$
18.   ELSE ($C_{\mathrm{opt}} \geq C_{\max} \geq C_{\min}$)
19.   OUTPUT segment $\langle t_D - t_s, C_{\max} \rangle$
20.   END IF
21.   Start a new segment at t_B: $t_s = t_D$, $t_e = t_D + 1$, $q = 0$
22.   ELSE
23.   Set $t_e = t_e^*$
24.   END IF
25.   Compute $C_{\max}$, t_B, $C_{\min}$, and t_D over $[t_S, t_e]$
26. UNTIL $t_S = N$
27. END Function.

The energy-efficient optimal smoothing algorithm considers the effect of the transmitter energy consumption, peak data rate, client buffer status, and queuing delay. It is a comprehensive energy-efficient algorithm.

E. Performance Comparison

In the section, we compare baseline transmission, frame-by-frame transmission (Section III-A), GOP-by-GOP transmission (Section III-B), the CBEVT algorithm (Section III-C), the smoothing algorithm (Section III-D), and the energy-efficient optimal smoothing algorithm (Section III-D) with respect to the data rate peak-to-mean ratio, standard deviation of the data rate, receiving energy per bit, transmission energy per bit, and total energy consumption per bit. We simulate the transmission schemes with three 30-minute VBR MPEG-4 quarter common interchange format encodings from the movie *Terminator 1* and one common interchange format encoding from the movie *Jurrassic Park 1*. The video streams with a range of bit rates are available at http://trace.eas.asu.edu, and their properties are summarized in Table IV. The system parameters are the same as in Table II. We run many independent replications of each simulation with random start points in the video streams until the 99% confidence level is less than 10% of the corresponding sample mean.

In the simulations in Tables V and VI, we compare the performance for Streams 2 and 4 for different buffer sizes for a start-up delay of $P = 2$ frames. Based on simulations with different P, we found that increasing P slightly reduces the peak-to-mean ratio and standard deviation while not significantly changing the energy performance based on the results that were reported in the following for $P = 2$. Table V shows that the CBEVT algorithm achieves the best performance, with energy

TABLE V
PERFORMANCE COMPARISON FOR DIFFERENT VIDEO TRANSMISSION SCHEMES FOR STREAM 2 WITH DIFFERENT CLIENT BUFFER SIZES
(THE DISTANCE IS 25 m, THE START-UP DELAY IS $P = 2$ TIME SLOTS, AND THE CONFIDENCE LEVEL IS 99%)

Stream 2		Peak to Mean Ratio	Std Dev of Data Rate	Receiving Energy per Bit (J)	Transmission Energy per Bit (J)	Total Energy per Bit (J)
Buffer Size = 128 KB	Baseline	14.22	1.33	9.10e-7	1.4e-7	1.05e-6
	Frame by Frame	14.92	14.88	9.10e-7	1.0e-7	1.01e-6
	GOP by GOP	14.92	14.80	9.10e-7	0.90e-7	1.00e-6
	Smoothing	2.74	0.27	9.10e-7	1.3e-7	1.04e-6
	En. eff. opt. sm.	2.76	0.28	9.10e-7	1.2e-7	1.03e-6
	CBEVT	14.81	3.72	9.06e-7	0.93e-7	9.99e-7
Buffer Size = 512 KB	Smoothing	1.28	0.15	9.10e-7	1.3e-7	1.03e-6
	En.. eff. opt. sm.	1.31	0.18	9.10e-7	1.2e-7	1.03e-6
	CBEVT	14.64	3.65	8.91e-7	0.92e-7	9.83e-7
Buffer Size = 2 MB	Smoothing	1.12	0.11	9.10e-7	1.3e-7	1.04e-6
	En.. eff. opt. sm.	1.13	0.11	9.10e-7	1.2e-7	1.03e-6
	CBEVT	13.74	3.41	8.38e-7	0.90e-7	9.28e-7
Buffer Size = 4 MB	Smoothing	1.05	0.11	9.10e-7	1.3e-7	1.03e-6
	En.. eff. opt. sm.	1.05	0.11	9.10e-7	1.2e-7	1.03e-6
	CBEVT	12.48	3.07	7.61e-7	0.90e-7	8.51e-7
Buffer Size = 16 MB	Smoothing	1.02	0.10	9.10e-7	1.3e-7	1.04e-6
	En.. eff. opt. sm.	1.03	0.11	9.10e-7	1.2e-7	1.03e-6
	CBEVT	7.01	1.64	4.20e-7	0.90e-7	5.11e-7

TABLE VI
PERFORMANCE COMPARISON FOR DIFFERENT VIDEO TRANSMISSION SCHEMES FOR STREAM 4 WITH DIFFERENT CLIENT BUFFER SIZES
(THE DISTANCE IS 25 m, THE START-UP DELAY IS $P = 2$ TIME SLOTS, AND THE CONFIDENCE LEVEL IS 99%)

Stream 4		Peak to Mean Ratio	Std Dev of Data Rate	Receiving Energy per Bit (J)	Transmission Energy per Bit (J)	Total Energy per Bit (J)
Buffer Size = 512 KB	Baseline	4.78	0.96	7.21e-8	9.38e-7	1.01e-6
	Frame by Frame	4.78	1.28	7.21e-8	2.17e-7	2.89e-7
	GOP by GOP	4.73	0.95	7.21e-8	1.47e-7	2.19e-7
	Smoothing	4.62	0.48	7.21e-8	1.53e-7	2.25e-7
	En.. eff. opt. sm.	4.62	0.50	7.21e-8	1.50e-7	2.22e-7
	CBEVT	4.72	0.73	7.20e-8	1.41e-7	2.13e-7
Buffer Size = 2 MB	Smoothing	4.15	0.39	7.21e-8	1.26e-7	1.98e-7
	En.. eff. opt. sm.	4.15	0.40	7.21e-8	1.24e-7	1.96e-7
	CBEVT	4.70	0.65	7.17e-8	1.19e-7	1.91e-7
Buffer Size = 4 MB	Smoothing	3.51	0.29	7.21e-8	1.12e-7	1.84e-7
	En.. eff. opt. sm.	3.51	0.30	7.21e-8	1.11e-7	1.83e-7
	CBEVT	4.66	0.54	7.11e-8	1.09e-7	1.80e-7
Buffer Size = 16 MB	Smoothing	2.13	0.09	7.21e-8	1.01e-7	1.73e-7
	En.. eff. opt. sm.	2.13	0.10	7.21e-8	1.00e-7	1.72e-7
	CBEVT	3.43	0.32	6.96e-8	9.24e-8	1.62e-7
Buffer Size = 32 MB	Smoothing	1.84	0.10	7.21e-8	9.89e-8	1.71e-7
	En.. eff. opt. sm.	1.84	0.10	7.21e-8	9.69e-8	1.69e-7
	CBEVT	2.67	0.25	6.51e-8	9.24e-8	1.58e-7
Buffer Size = 64 MB	Smoothing	1.37	0.07	7.21e-8	9.69e-8	1.69e-7
	En.. eff. opt. sm.	1.37	0.08	7.21e-8	9.59e-8	1.68e-7
	CBEVT	1.02	0.22	6.16e-8	9.24e-8	1.54e-7

savings of up to 51% compared with the baseline transmission for Stream 2 when the buffer size is 16 MB. In Table VI, we observe energy savings of up to 85% for Stream 4, with a buffer size of 64 MB. We also see that the CBEVT energy performance improves with an increasing buffer size. More specifically, we observe in Table V that for a stream with a low bit rate (relative to $C_{\text{opt}} = 2$ Mb/s), for a small buffer,

the energy savings mainly comes from the transmission energy component, whereas for large buffer sizes, the savings mainly comes from the receiving energy component. For instance, when the buffer size is 128 KB, 92% of the energy savings comes from the transmission component, and only 7.8% comes from the receiving component. When the buffer size increases to 16 MB, the transmission savings component, which stays

constant for growing buffer sizes, is 9.2%, and the receiving component is 91%. These observations can be explained by two main facts. First, the considered common client buffers are sufficiently large to allow the transmission of essentially all video frames of the low-bit-rate stream at the optimal data rate C_{opt} according to (11). Second, $C_{opt} = 2$ Mb/s is larger than the average bit rate of Stream 2; therefore, the transmission at C_{opt} prefetches video frames into the receiver buffer until it is completely filled, and the left inequality in (11) is violated. The larger the receiver buffer capacity is, the sooner that all frames of the 30-min video stream can be prefetched, i.e., the shorter the active time becomes. Hence, a large buffer reduces the receive energy consumption in the transceiver by completing the transmission of the entire video in less time. Further increases in the buffer size will further reduce the receive energy consumption. When the receive buffer can essentially hold the entire video, no further receive energy reductions are achieved by further increasing the receiver buffer.

Turning to the higher bit rate Stream 4, we observe in Table VI that, for small buffer sizes, the energy savings are mainly due to reduced transmission energy. With a growing buffer size, the transmission energy further decreases, whereas the reception energy also decreases. For this higher bit rate stream, larger buffers allow more transmissions at C_{opt}, which results in the drop of the transmission energy to 9.24e-8 J per bit for a 16-MB buffer. Further increases in the buffer size do not result in further transmission energy reductions, because, in essence, all transmissions are at C_{opt} for the 16-MB buffer. On the other hand, the reception energy continues to drop for increasing buffer sizes as larger buffer sizes decrease instances of stalling.

The original optimal smoothing algorithm [14] has the best performance in terms of reducing the video peak-to-mean ratio and standard deviation of the transmission rates. However, its energy saving performance is poor (i.e., less than 1%) for the lower bit rate stream, whereas it gives a good energy performance for the higher bit rate stream, because the smoothing algorithm [14] was designed to minimize bit rate variations around the average bit rate. If the average bit rate is far from C_{opt}, transmissions according to the smoothed rates require high energy (e.g., for Stream 2), whereas energy is saved if the average rate is close to C_{opt} (e.g., for Stream 4). The energy-efficient optimal smoothing algorithm achieves a mild improvement in energy performance (i.e., it saves about 2%) over optimal smoothing by minimizing the transmission energy while achieving essentially the same rate smoothing as optimal smoothing.

For Stream 2, we observe in Table V that frame-by-frame and GOP-by-GOP transmission save around 4% of energy compared with the baseline transmission but have high peak-to-mean ratios, which are only slightly smaller for the GOP-by-GOP transmission. Note that, for Stream 2 with a peak rate below C_{opt}, the frame-by-frame and GOP-by-GOP transmission accelerate the data rate to C_{opt}, thus increasing the peak-to-mean ratio and standard deviation of the transmission rate compared to the baseline transmission. All frame data is transmitted at the optimal data rate, so the transmission energy of the frame-by-frame, GOP-by-GOP, and CBEVT transmission

is, within the statistical reliability of the simulation, the same. However, the frame-by-frame and GOP-by-GOP transmission have the same receiving energy as the baseline transmission. Note that, in Tables V and VI, we report results for the baseline, frame-by-frame, and GOP-by-GOP transmission only for the smallest buffer sizes, which are large enough to accommodate the maximum GOP size, i.e., about 81 KB for Stream 2 and 391 KB for Stream 4.

For the higher rate Stream 4, we observe in Table VI that the frame-by-frame and GOP-by-GOP transmission significantly reduce the transmission energy compared to the baseline transmission, but they do not achieve the low transmission energies that the smoothing schemes and CBEVT reach for large buffers. The transmission energy savings of the frame-by-frame and GOP-by-GOP transmission come from speeding up the transmission of frames that are smaller than $C_{opt} \times T_{frame}$; therefore, they are transmitted at C_{opt} within less than one frame period and similarly for GOPs. Frames that are larger than $C_{opt} \times T_{frame}$ are transmitted at a rate higher than C_{opt} to complete transmission within one frame period. These higher rate transmissions are, to a large degree, avoided by the smoothing and CBVET schemes.

Next, we evaluate the effect of different data rates by considering the four representative video streams. The simulation results are shown in Table VII. We observe that, with an increasing data rate (from Stream 1 to Stream 4), the total RF energy consumption per bit decreases. More specifically, we observe significant drops in the receiving energy for all transmission strategies, including the baseline transmission. The reason for this decreasing receive energy consumption with higher stream bit rates is that, within approximately the same active time, more bits are received, which results in a lower receiving energy per bit.

The CBEVT algorithm has superior energy performance for all the four streams. The peak-to-mean ratio of CBEVT for Stream 1 is equal to 1, because the client buffer is large enough to hold the entire video; thus, all the frames are continuously transmitted at the optimal data rate C_{opt}. With an increasing video data rate, the peak-to-mean ratio of the GOP-by-GOP transmission decreases more compared to the frame-by-frame transmission. For example, for Stream 3, the GOP-by-GOP transmission reduces the peak-to-mean ratio by 42.6%, whereas the frame-by-frame transmission reduces it by about 13.9%, because the GOP-by-GOP scheme considers 12 frames as one unit, and the large frame sizes (high data rates) are balanced by the small frames in the same GOP.

IV. ENERGY-EFFICIENT VIDEO TRANSMISSION FOR CDMA-BASED MULTIUSER SYSTEMS

In this section, we first describe an improved RF front-end energy model that considers MAI. Then, we propose the MBEVT algorithm and evaluate its energy and quality performance. We consider a single cell of a CDMA-based multiuser wireless system with perfect power control, orthogonal PN sequences for the different users, and M-QAM, as these factors are likely characteristics of future metropolitan-scale Wi-Fi networks.

TABLE VII
PERFORMANCE COMPARISONS FOR DIFFERENT VIDEO STREAMS WITH A 16-MB CLIENT BUFFER (THE DISTANCE IS 25 m,
THE START-UP DELAY IS $P = 2$ TIME SLOTS, AND THE CONFIDENCE LEVEL IS 99%)

Buffer Size = 16 MB		Peak to Mean Ratio	Std Dev of Data Rate	Receiving Energy per Bit (J)	Transmission Energy per Bit (J)	Total Energy per Bit (J)
Stream 1	Baseline	8.42	0.70	1.98e-6	1.4e-7	2.12e-6
	Frame by Frame	32.46	32.44	1.98e-6	0.90e-7	2.07e-6
	GOP by GOP	32.46	32.44	1.98e-6	0.90e-7	2.07e-6
	Smoothing	1.55	0.07	1.98e-6	1.3e-7	2.11e-6
	En. eff. opt. sm.	1.57	0.08	1.98e-6	1.1e-7	2.09e-6
	CBEVT	1.00	0.08	6.11e-8	0.90e-7	1.51 e-7
Stream 2	Baseline	14.22	1.33	9.10e-7	1.4e-7	1.05e-6
	Frame by Frame	14.92	14.88	9.10e-7	1.0e-7	1.01e-6
	GOP by GOP	14.92	14.80	9.10e-7	0.90e-7	1.00e-6
	Smoothing	1.02	0.10	9.10e-7	1.3e-7	1.04e-6
	En. eff. opt. sm.	1.03	0.11	9.10e-7	1.2e-7	1.03e-6
	CBEVT	7.01	1.64	4.20e-7	0.90e-7	5.11e-7
Stream 3	Baseline	11.7	0.95	4.10e-7	1.39e-7	5.49e-7
	Frame by Frame	10.08	6.64	4.10e-7	0.93e-7	5.03e-7
	GOP by GOP	6.72	6.64	4.10e-7	0.92e-7	5.02e-7
	Smoothing	1.44	0.11	4.10e-7	1.04e-6	5.41e-7
	En. eff. opt. sm.	1.45	0.12	4.10e-7	1.01e-6	5.38e-7
	CBEVT	4.99	1.65	3.04e-7	0.90e-7	3.93e-7
Stream 4	Baseline	4.78	0.96	7.21e-8	9.38e-7	1.01e-6
	Frame by Frame	4.78	1.28	7.21e-8	2.17e-7	2.89e-7
	GOP by GOP	4.73	0.95	7.21e-8	1.47e-7	2.19e-7
	Smoothing	2.13	0.09	7.21e-8	1.01e-7	1.73e-7
	En. eff. opt. sm.	2.13	0.10	7.21e-8	1.00e-7	1.72e-7
	CBEVT	3.43	0.32	6.96e-8	9.24e-8	1.62e-7

A. RF Front-End Energy Model in Multiuser Systems

In the single-user system, the transmitter energy consumption is evaluated for a constant BER of 10^{-3}. Thus, the communication quality is fixed. If the channel Gaussian noise power is constant in one time slot, the detected power P_{detected} must be changed with the modulation level b to maintain the BER. Thus, in the single-user system, the SNR varies with the modulation level b.

However, in CDMA-based multiuser systems with perfect power control, the power control ensures that the signal-to-interference-noise ratio (SINR) for every wireless uplink is the same. (Here, the signal suffers from interference due to both Gaussian noise and MAI.) Thus, the BERs vary with the modulation level b, and the method that was derived for the single-user system cannot directly be used in multiuser systems. Therefore, the transmitter energy model must be adjusted for the multiuser system with a fixed SINR.

Recall that the SINR is defined as $\text{SINR} = (A \cdot P_{\text{detected}})/(N_W + A \cdot N_{\text{MAI}})$, where A is the attenuation factor, which is constant during a frame time in the slow-fading channel, $N_w \sim (0, N_0/2)$ is the Gaussian noise in the additive white Gaussian noise channel, and $N_{\text{MAI}} \sim (0, ((S-1)/(2 \cdot \text{PN}))E_{\text{ave}} \cdot (1 - (\alpha/4)))$ is the MAI that is typically approximated by a Gaussian distribution [23], [24]. Here, S is the number of users in the cell, PN is the length of the pseudonoise sequence, E_{ave} is the average signal energy per symbol, and α is the roll-off factor of the raised cosine pulse-shaping filter. After the signal passes through the pulse-shaping filter, the bandwidth increases

to $\text{BW} = 1/2 \cdot R_s \cdot (1 + \alpha)$ [25]. For perfect power control, the power level of every user is equal. Thus

$$
\begin{aligned}
\text{SINR} &= \frac{A \cdot P_{\text{detected}}}{N_0 \cdot \text{BW} + A \cdot \frac{S-1}{\text{PN}} E_{\text{ave}} \cdot \left(1 - \frac{\alpha}{4}\right) \cdot \text{BW}} \\
&= \frac{A \cdot P_{\text{detected}}}{N_0 \cdot \text{BW} + A \cdot \frac{S-1}{2 \cdot \text{PN}} P_{\text{detected}} \cdot \left(1 - \frac{\alpha}{4}\right) \cdot (1 + \alpha)}.
\end{aligned}
\tag{17}
$$

Hence

$$
P_{\text{detected}} = \frac{2 \cdot \text{SINR} \cdot \text{PN} \cdot N_0 \cdot R_s \cdot (1 + \alpha)}{2 \cdot A \cdot \text{PN} - (S-1) \cdot A \cdot \text{SINR} \cdot (1 - 0.25\alpha)(1 + \alpha)}.
$$

Based on the aforementioned equations, the transmitter energy consumption for a single bit is given by (18), shown at the bottom of the next page.

The relation between the energy per bit and the modulation level b for a given SINR is illustrated in Fig. 5. For a given SINR, the energy per bit decreases as the modulation level b increases. Thus, for low-power video transmission, a high data rate (i.e., a large modulation level) is preferred. Reducing the SINR in the single-user system is also a good way to decrease the transmitter energy consumption. Although Fig. 5 shows the relation when the distance $d = 3$ m, the trend is similar for other values of d. Note that the trend is different in Fig. 3, because the BER is a variable in Fig. 5 (compared with the constant BER
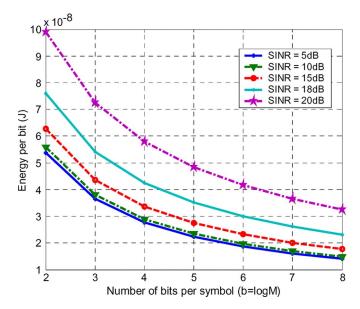
Fig. 5. Energy per bit for different modulation levels b under different SINRs (the number of users is $S = 15$, and $d = 3$ m).

Fig. 6. Bit error rate for different modulation levels b under different SINRs (the number of users in the cell is 15).

TABLE VIII
MINIMUM SINR FOR DIFFERENT MODULATION LEVELS b, BER $\leq 10^{-3}$

b	2	3	4	5	6	7	8
SINR(dB)	9.8	13.4	16.5	19.6	22.5	25.5	28.4

in Fig. 3), and the SINR is a constant. For the same SINR, a higher modulation level results in lower energy consumption per bit.

B. SINR and BER in Multiuser Systems

In a CDMA-based multiuser communication system, the BER is not constant, because the modulation level is adaptive, and the data rate is scalable. However, the BER value must be smaller than a preset threshold to guarantee that the FEC can correct the errors and avoid the retransmission of video frames. In this section, we assume that the BER is equal to or smaller than 10^{-3}, i.e.,

$$\text{BER} = \frac{4}{b}\left(1 - \frac{1}{2^{b/2}}\right) \cdot Q\left(\sqrt{\frac{3\text{SINR}}{(2^b - 1)}}\right) \leq 10^3. \quad (19)$$

Based on (19) [25], we can generate the curves for BER versus the modulation level b for a different SINR, as shown in Fig. 6. Once the BER constraint is known, we can use Figs. 5 and 6 to determine the optimal combination of (b, SINR), which corresponds to the lowest transmission energy. For example, if the BER constraint is 10^{-3}, based on Fig. 6, the (b, SINR) combinations that satisfy the BER requirement are (2, 10 dB), (2, 15 dB), (2, 18 dB), (2, 20 dB), (3, 15 dB), (3, 18 dB), (3, 20 dB), (4, 18 dB), (4, 20 dB), and (5, 20 dB). For these combinations, we use Fig. 5 to find that the combination (4,
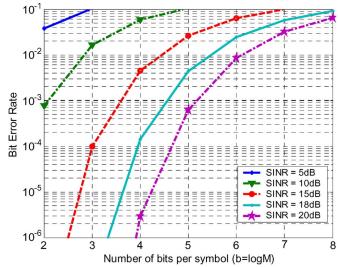
18 dB) is the most energy-efficient configuration when the distance is $d = 3$ m.

The aforementioned method can be generalized for finding the most energy efficient combination of (b, SINR) for a given distance d. We first utilize (19) with the BER threshold 10^{-3} to obtain

$$\text{SINR} = \frac{1}{3}(2^b - 1) \cdot \left(Q^{-1}\left(\frac{1}{4}\left(1 - \frac{1}{2^{b/2}}\right)^{-1} \cdot b \cdot 10^3\right)\right)^2. \quad (20)$$

Based on (20), we can generate Table VIII, which shows the value of the minimum SINR for a given modulation level b. Intuitively, as the modulation level of the transmitter increases (i.e., the data rate increases), the receiver is more sensitive to the channel noise and the MAI. Therefore, the minimum $SINR$ must increase to maintain the required BER. This has also been graphically shown in Fig. 6. The combinations of (b, SINR) in Table VIII are the candidates for the optimal configuration. Note that the optimal combination of (b, SINR) varies with the distance d.

$$E_{\text{bit}} = (P_{\text{PA}} + P_{\text{RF}}) \cdot \frac{1}{b \cdot R_s} = \frac{107 \times 10^{-3}}{b \cdot R_s} + \frac{16 \cdot \pi^2 \cdot d^2 \cdot L}{G_r G_t \lambda^2 \cdot K \cdot b \cdot R_s} P_{\text{detected}} \cdot \text{PAR}(b)$$

$$= \frac{107 \times 10^{-3}}{b \cdot R_s} + \frac{32 \cdot \pi^2 \cdot d^2 \cdot L \cdot \text{PAR}_C \cdot \text{PAR}_{\text{roll-off}} \cdot \text{SINR} \cdot \text{PN} \cdot N_0 \cdot (1+\alpha)}{G_r G_t \lambda^2 \cdot K \cdot b \cdot A \cdot (2 \cdot \text{PN} - (S-1) \cdot \text{SINR} \cdot (1 - 0.25\alpha)(1+\alpha))} \cdot \sqrt{\frac{3 \cdot (2^{b/2} - 1)}{(2^{b/2} + 1)}} \quad (18)$$

To find the configuration with a minimum E_{bit} for a given d, we compute the E_{bit} for every combination of (b, SINR) (see Table VIII) using (18) and choose the configuration with the minimum E_{bit}.

In a multiuser scenario, every user in the cell is likely to be at a different distance from the base station. However, perfect power control in the CDMA system ensures that the SINR in every link is always kept the same. The optimal combination of (b, SINR) for every user varies with the distance, so the optimal combination of (b, SINR) for the entire cell must be evaluated and chosen from all the possible (b, SINR) combinations. We determine the optimal combination of (b, SINR) for the cell as the minimum sum of E_{bit} over all users.

Suppose that S is the number of users in the cell, and $(b_{\text{opt}\_i}, \text{SINR}_{\text{opt}\_i})$ is the optimal combination for user i $(i = 1, 2, \ldots, S)$ with distance d_i. Define $E_{i,j}$ as the energy consumption of user j if the operating parameters are $(b_{\text{opt}\_i}, \text{SINR}_{\text{opt}\_i})$. Then, the optimal combination of $(b_{\text{opt}}, \text{SINR}_{\text{opt}})$ for the entire system corresponds to $\min_i(\sum_{j=1}^{S} E_{i,j})$.

C. MBEVT Algorithm

In Sections IV-A and B, we find that, once the optimal SINR is determined in the CDMA system, a higher modulation level b (i.e., a higher data rate) results in lower transmitter energy consumption. Furthermore, with a higher data rate, the video transmission finishes earlier, which results in the transceiver staying in the sleep mode and, thus, saving energy. However, the transmission data rate must be considered with the buffer occupancy in the client and the BER threshold. If the data rate (i.e., the modulation level) is too high, the client buffer may overflow, and the BER may exceed the threshold.

If the number of the active users in the cell is smaller, the MAI is smaller, and, thus, the transmission power that is needed to maintain the preset SINR is lower. If the client buffer has enough frames to continue playback for the following time slots, the transmitter can be suspended until the client buffer occupancy drops. As a result, the number of active users (or the MAI) in the cell decreases, and the energy that the active transmitters consume also decreases.

Next, we develop the MBEVT algorithm, which strives to reduce the energy consumption by transmitting at a high data rate and putting the transmitter into the idle mode, thus reducing the number of active users. The basic idea of the algorithm is that the video frames are transmitted at the maximum possible data rate (i.e., modulation level b) that satisfies the BER constraint and the buffer starvation and overflow constraints $\sum_{i=1}^{k} L(i) \leq \sum_{i=1}^{k-1} a(i) + a(k) \leq Buffer + \sum_{i=1}^{k-1} L(i)$. Here, we set the start-up delay to $P = 1$ time slot, and all the parameter definitions are still the same. We consider the threshold policy that, if the amount of data in the client buffer reaches t_h of its capacity, the transmitter suspends until the client buffer occupancy is less than t_l of the buffer capacity. The thresholds (t_h, t_l) can be adjusted according to the client buffer size. For the numerical examples in this paper, we set $t_h = 0.8$ and $t_l = 0.2$. Determining the optimal threshold criterion is left for future work.

MBEVT function: find optimal schedule $(a(t), Buffer)$

1.   *Check Table VIII for the combination of $(b_i, SINR_i)$*
2.   *For $i = 1 : S$ /* number of users in the system*
3.   *For $j = 1 : 7$ /* 7 is the number of possible b values, $b \in [2, 8]$*
4. $E_{bit}(i, j) = f(b_j, SINR_j, d_i)$
5.   *end*
6. $E_{bit\_opt}(i) = min\{E_{bit}(i, :)\}$;   *Find the corresponding $(b_{i\_opt}, SINR_{i\_opt})$*
7.   *end*
8.   *For $i = 1 : S$*
9.   *For $j = 1 : S$*
10. $E_{temp}(i, j) = f(b_{i\_opt}, SINR_{i\_opt}, d_j)$
11.   *end*
12. $E(i) = \sum(E_{\text{temp}}(i, :))$
13.   *end*
14. $E_{opt} = min(E(:))$; *Find the corresponding $E_{opt} => (b_{opt}, SINR_{opt})$*
15. $C_{opt} = b_{opt} \times R_s$; $T_{\text{frame}} = 33 \times 10^{-3}$ sec
16.   *For $i = 1 : N$*
17.   *For $j = 1 : S$*
18. $\text{Re}main\_buffer(i) = \sum_{k=1}^{i-1} a(j, k) - \sum_{k=1}^{i} L(j, k)$
19.   *if* $(\text{Re}main\_buffer(i) \geq t_h \times Buffer)$
20.   *Repeat*
21.   *OUTPUT frame* $\langle a(j, i), 0 \rangle$
22. $i = i + 1$
23.   *End until* $(\text{Re}main\_buffer(i) \leq t_l \times Buffer)$
24.   *Else if*

$$\sum_{k=1}^{i-1} a(j, k) + a(j, i)$$

$$\leq \min\left\{ Buffer + \sum_{k=1}^{i-1} L(j, k), \sum_{k=1}^{i-1} a(j, k) + C_{opt} \cdot T_{frame} \right\}$$

25.   *OUTPUT frame*

$$\left\langle a(j, k), \min\left\{ Buffer + \sum_{k=1}^{i-1} L(j, k) - \sum_{k=1}^{i-1} a(j, k), C_{\text{opt}} \cdot T_{\text{frame}} \right\} \right\rangle$$

26.   *end if*
27.   *End*
28.   *End*
29.   *END Function*

To evaluate the performance of the MBEVT algorithm, we simulate a CDMA-based multiuser wireless environment. The number of users in the cell is $S = 6$. Every user starts the video transmission at randomly chosen video frames. The mobile users are randomly located in the cell, and the average distance is about 17 m. We use M-QAM for the video transmission, which is susceptible to interference; therefore, a 2047-PN sequence is adopted. The other simulation parameters and video traces [26] are the same (see Tables I and II). We use Stream 2, because it has a data rate that is comparable with today's typical wireless transmission speeds. We run enough independent

TABLE IX
MBEVT ALGORITHM PERFORMANCE COMPARISONS FOR DIFFERENT BUFFER SIZES (E_{bit} IS THE AVERAGE ENERGY CONSUMPTION FOR THE
SIX USERS, THE PEAK-TO-MEAN RATIO IS THE MAXIMUM VALUE FOR THE SIX USERS; THE BASELINE SCHEME IS THE SAME
AS IN SECTION III-E, AND THE SIX USERS INDEPENDENTLY EMPLOY THE BASELINE SCHEME)

Buffer	128KB	256KB	512KB	1MB	2MB	4MB	8MB	16MB	Baseline
E_{bit}(e-7J)	8.82	8.81	8.76	8.73	8.45	7.92	7.88	6.26	10.08
Max Peak to Mean Ratio	22.36	22.35	22.30	22.28	22.13	21.93	20.71	17.49	14.22
Active num of users	4.94	4.95	4.96	4.96	4.98	5.06	5.06	5.25	6

replication so that our simulation data has a confidence level of 90%, which is less than 10% of the sample mean.

Table IX shows that the MBEVT algorithm reduces the energy consumption and the average active number of users in the cell while increasing the peak-to-mean ratio compared with the baseline scheme. The average energy consumption and the maximum peak-to-mean ratio decrease with an increasing buffer size. For instance, if the client buffer size increases from 128 KB to 16 MB, the energy savings increases from 12.5% to 37.9%. If we have a larger buffer size, the transmitter can operate at a higher data rate, which increases the possibility that the transmitter will work at the system optimal data rate. Furthermore, since the peak data rate is always constrained by the BER requirement and is independent of the buffer size, a higher average data rate results in a lower video transmission peak-to-mean ratio. However, with the increase in the client buffer size, the average number of active users in the cell also increases, because the buffer occupancy threshold (i.e., $t_h = 0.8$ in our simulation) is harder to reach due to the larger buffer size. Although the total transmission time is reduced, a slightly larger number of mobile users are active in the same time slot, and the MAI mildly increases. Based on this analysis, we conclude that the effect of a higher data rate is larger for energy savings than the minor increase in the average active number of users in the cell (i.e., higher MAI).

V. CONCLUSION

We have presented multiple energy-efficient transmission schemes for prerecorded continuous media (e.g., streaming video and audio) in single-user and multiuser systems. The energy efficiency is obtained by adjusting parameters in the PHY and MAC layers. For a single-user system, we have presented three energy-efficient schemes: 1) the frame-by-frame transmission; 2) the GOP-by-GOP transmission; and 3) the CBEVT. We have also presented a modified version of the optimal smoothing algorithm to reduce both the peak data rate and the RF front-end energy consumption. Our simulation results indicate that, for video streams with bit rates below the transmission rate that corresponds to the energy-minimizing modulation level, the frame-by-frame transmission, GOP-by-GOP transmission, and CBEVT achieve the minimum transmission energy consumption. In addition, CBEVT reduces the reception energy consumption by completing the video trans-

mission sooner and, thus, achieves the lowest energy consumption among the considered schemes. For video streams with peak bit rates that frequently exceed the transmission rate that corresponds to the energy-minimizing modulation level, the smoothing strategies can achieve low energy consumption if the average bit rate of the video is close to the energy-minimizing transmission rate and the receiver buffer is sufficiently large. Across all the examined video bit rates and receiver buffer sizes, CBEVT achieves the smallest energy consumption among the studied strategies. For the CDMA-based multiuser system, we have proposed a new RF front-end energy model and the corresponding MBEVT algorithm to reduce the energy consumption. Our simulation results indicate that the energy savings for a multiuser system comes with a lower number of active users (i.e., lower MAI) and higher peak data rate.

In the future, we plan to consider the effect of the source coding block on the energy and QoS performance. We also plan to study low-power OFDM technology for high-definition wireless videos.

REFERENCES

[1] M. Srivatsava, "Power-aware communication systems," in *Power-Aware Design Methodologies*, M. Pedram and J. M. Rabaey, Eds. Norwell, MA: Kluwer, 2002, ch. 11.
[2] Y. Li, B. Bakkaloglu, and C. Chakrabarti, "A system-level energy model and energy-quality evaluation for integrated transceiver front ends," *IEEE Trans. Very Large Scale Integr. (VLSI) Syst.*, vol. 15, no. 1, pp. 90–103, Jan. 2007.
[3] Y. Li, B. Bakkaloglu, and C. Chakrabarti, "Comprehensive energy model and energy-quality evaluation for wireless transceiver front end," in *Proc. IEEE Workshop SiPS*, Nov. 2005, pp. 262–267.
[4] B. Razavi, *RF Microelectronics*. Upper Saddle River, NJ: Prentice–Hall, 1998.
[5] S. Cui, A. J. Goldsmith, and A. Bahai, "Energy-constrained modulation optimization," *IEEE Trans. Wireless Commun.*, vol. 4, no. 5, pp. 2349–2360, Sep. 2005.
[6] B. Prabhakar, E. U. Biyikoglu, and A. E. Gamal, "Energy-efficient transmission over a wireless link via lazy packet scheduling," in *Proc. of IEEE INFOCOM*, Apr. 2001, pp. 386–394.
[7] X. Lu, E. Erkip, Y. Wang, and D. Goodman, "Power-efficient multimedia communication over wireless channel," *IEEE J. Sel. Areas Commun.*, vol. 21, no. 10, pp. 1738–1751, Dec. 2003.
[8] Il.-M. Kim and H. Kim, "Power-distortion optimized mode selection for transmission of VBR videos in CDMA systems," *IEEE Trans. Commun.*, vol. 51, no. 4, pp. 525–529, Apr. 2003.
[9] Il.-M. Kim and H. Kim, "Transmit power optimization for video transmission over slow-varying Rayleigh- fading channels in CDMA systems," *IEEE Trans. Wireless Commun.*, vol. 3, no. 5, pp. 1411–1415, Sep. 2004.
[10] X. Lu, Y. Chen, and Y. Wang, "Joint PHY and MAC layer power optimization for video transmission over wireless LAN," in *Proc. SPIE, VCIP*, Jan. 2004, pp. 110–118.

[11] X. Lu, Y. Wang, E. Erkip, and D. Goodman, "Minimize the total power consumption for multiuser video transmission over CDMA wireless network: A two-step approach," in *Proc. IEEE ICASSP*, 2005, pp. 941–944.

[12] Q. Zhang, Z. Ji, W. Zhu, and Y. Zhang, "Power-minimized bit allocation for video communication over wireless channels," *IEEE Trans. Circuits Syst. Video Technol.*, vol. 12, no. 6, pp. 398–409, Jun. 2002.

[13] C. E. Luna, Y. Eisenberg, R. Berry, T. N. Pappas, and A. K. Katsaggelos, "Joint source coding and data rate adaptation for energy efficient wireless video streaming," *IEEE J. Sel. Areas Commun.*, vol. 21, no. 10, pp. 1710–1720, Dec. 2003.

[14] J. D. Salehi, Z. Zhang, J. Kurose, and D. Towsley, "Supporting stored video: Reducing rate variability and end-to-end resource requirements through optimal smoothing," *IEEE/ACM Trans. Netw.*, vol. 6, no. 4, pp. 397–410, Aug. 1998.

[15] S. Pollin, R. Mangharam, B. Bougard, L. Van der Perre, I. Moerman, R. Rajkumar, and F. Catthoor, "MEERA: Cross-layer methodology for energy efficient resource allocation in wireless networks," *IEEE Trans. Wireless Commun.*, vol. 6, no. 2, pp. 617–628, Feb. 2007.

[16] J. Yeh, J. Chen, and C. Lee, "Comparative analysis of energy saving techniques in 3GPP and 3GPP2 systems," *IEEE Trans. Veh. Technol.*, 2008. to be published.

[17] M. Gustavsson, J. J. Wikner, and N. N. Tan, *CMOS Data Converters for Communications*. Norwell, MA: Kluwer, 2000.

[18] C. Schurgers, V. Raghunathan, and M. B. Srivastava, "Power management for energy-aware communication systems," *ACM Trans. Embed. Comput. Syst. (TECS)*, vol. 2, no. 3, pp. 431–447, Aug. 2003.

[19] C. M. Assi, A. Agarwal, and Y. Liu, "Enhanced per-flow admission control and QoS provisioning in IEEE 802.11e wireless LANs," *IEEE Trans. Veh. Technol.*, vol. 57, no. 2, pp. 1077–1088, Mar. 2008.

[20] G. Boggia, P. Camarda, L. A. Grieco, and S. Mascolo, "Feedback-based control for providing real-time services with 802.11e MAC," *IEEE Trans. Netw.*, vol. 15, no. 2, pp. 323–333, Apr. 2007.

[21] S. Shankar and M. van der Schaar, "Performance analysis of video transmission over IEEE 802.11a/e WLANs," *IEEE Trans. Veh. Technol.*, vol. 56, no. 4, pp. 2346–2362, Jul. 2007.

[22] Y. Xiao and Y. Pan, "Differentiation, QoS guarantee, and optimization for real-time traffic over one-hop ad hoc networks," *IEEE Trans. Parallel Distrib. Syst.*, vol. 16, no. 6, pp. 538–549, Jun. 2005.

[23] G. Zang and C. Liang, "Performance evaluation for band-limited DS-CDMA system based on simplified improved Gaussian approximation," *IEEE Trans. Commun.*, vol. 51, no. 7, pp. 1204–1212, Jul. 2003.

[24] J. M. Holtzman, "A simple, accurate method to calculate spread-spectrum multiple-access error probabilities," *IEEE Trans. Commun.*, vol. 40, no. 3, pp. 461–464, Mar. 1992.

[25] T. S. Rappaport, *Wireless Communications Principles and Practice*. Upper Saddle River, NJ: Prentice–Hall, 1996.

[26] P. Seeling, M. Reisslein, and B. Kulapala, "Network performance evaluation with frame size and quality traces of single-layer and two-layer video: A tutorial," *Commun. Surveys Tuts.*, vol. 6, no. 3, pp. 58–78, Third Quarter 2004.

Ye Li received the B.S. and M.S. degrees in electrical engineering from the University of Electronic Science and Technology of China, Chengdu, China, in 1999 and 2002, respectively, and the Ph.D. degree in electrical engineering from Arizona State University, Tempe, in 2006.

In 2007, he was an Intern with Cadence Design Systems Inc., San Jose, CA. Since 2008, he has been an Assistant Professor with the Institute of Biomedical and Health Engineering, Shenzhen Institute of Advanced Technology (SIAT), Chinese Academy of Sciences, Shenzhen, China, where he is also the Executive Director of the Center for Biomedical Information Technology. His research interests include low-power wireless system design, sensor communication protocol design, and biomedical IC design.

Dr. Li was a Reviewer for the *Proceedings of the Fifth IEEE-EMBS International Conference on Information Technology and Applications in Biomedicine*, the *Second International Symposium and Summer School on Biomedical and Health Engineering (ITAB/IS3BHE'08)*, the *Proceedings of the Fifth International Workshop on Wearable and Implantable Body Sensor Networks*, and the *Fifth International Summer School and Symposium on Medical Devices and Biosensors (BSN/ISSS-MDBS'08)*.

Martin Reisslein (S'97–A'96–M'98–SM'03) received the Dipl.Ing. (FH) degree in electrical engineering from the Fachhochschule Dieburg, Dieburg, Germany, in 1994 and the M.S.E. degree in electrical engineering and the Ph.D. degree in systems engineering from the University of Pennsylvania, Philadelphia, in 1996 and 1998, respectively.

From 1994 to 1995, he visited the University of Pennsylvania as a Fulbright Scholar. From July 1998 to October 2000, he was a Scientist with the German National Research Center for Information Technology (GMD FOKUS), Berlin, Germany, and a Lecturer with the Technical University of Berlin. From October 2000 to August 2005, he was an Assistant Professor with the Arizona State University, Tempe, where he is currently an Associate Professor with the Department of Electrical Engineering. He maintains an extensive library of video traces for network performance evaluation, including frame-sized traces of MPEG-4 and H.264 encoded video, which are available at http://trace.eas.asu.edu. His research interests include Internet quality of service, video traffic characterization, wireless networking, optical networking, and engineering education.

Dr. Reisslein was the Editor-in-Chief of the IEEE COMMUNICATIONS SURVEYS AND TUTORIALS from January 2003 to February 2007. He has served on the Technical Program Committees of IEEE INFOCOM, IEEE GLOBECOM, and numerous other networking and engineering education conferences.

Chaitali Chakrabarti (SM'02) received the B.Tech. degree in electronics and electrical communication engineering from the Indian Institute of Technology, Kharagpur, India, in 1984 and the Ph.D. degree in electrical engineering from the University of Maryland, College Park, in 1990.

She is currently a Professor with the Department of Electrical Engineering, Arizona State University (ASU), Tempe. In 1999, she was an Associate Editor of the *Journal of VLSI Signal Processing Systems*. Her research interests include low-power embedded system design, in particular, memory optimization and compilation, VLSI architectures and algorithms for signal processing, image processing, communications, and algorithm-architecture codesign.

Dr. Chakrabarti received the Research Initiation Award from the National Science Foundation in 1993, the Best Teacher Award from the College of Engineering and Applied Sciences, ASU, in 1994, and the Outstanding Educator Award from the IEEE Phoenix Section in 2001. She has served on the Program Committees of the IEEE International Conference on Acoustics, Speech, and Signal Processing (ICASSP), the IEEE International Symposium on Circuits and Systems (ISCAS), the IEEE Workshop on Signal Processing Systems (SIPS), the International Symposium on High-Performance Computer Architecture (HPCA), the International Symposium on Low-Power Electronics and Design (ISLPED), and the Design Automation Conference (DAC). In 2007, she was an Associate Editor of the IEEE TRANSACTIONS ON VERY LARGE SCALE INTEGRATION (VLSI) SYSTEMS. From 1999 to 2004, she was the Associate Editor for the IEEE TRANSACTIONS ON SIGNAL PROCESSING. From 2006 to 2007, she was the Chair of the Subcommittee on Design and Implementation of Signal Processing Systems, Technical Committee, IEEE Signal Processing Society.